Journal of Energy Technologies and Policy
ISSN 2224-3232 (Paper) ISSN 2225-0573 (Online)
Vol.3, No.5, 2013

Design Optimization of Bifacial Solar Cell by PC1D Simulation

Suhaila Sepeai, Saleem H.Zaidi, M.K.M.Desa, M.Y.Sulaiman, N.A.Ludin, M.Adib Ibrahim, K.Sopian
Solar Energy Research Institute (SERI), Universiti Kebangsaan Malaysia (UKM), 43600 Bangi, Selangor, Malaysia
* E-mail of the corresponding author: suhaila_sepeai@yahoo.com

Abstract
In this study, design and optimization of bifacial solar cell was done with PC-1D simulation program. The influence of various parameters such as emitter doping, bulk doping, minority carrier lifetime, wafer thickness, front and rear surface recombination and illumination from front and rear surfaces were investigated using PC1D software simulation. The efficiencies obtained from this design were 16.42 % and 14.18 % for front and back surfaces, respectively. The results from these simulation studies prove that it is possible to propose these design parameters for bifacial solar cell fabrication. Our results also provide critical insight regarding fabrication of bifacial solar cells on good or poor quality Si wafers. From this study, it was found that minority carrier lifetime and wafer thickness are critical parameters to bifacial solar cell performance.
Keywords: Silicon, Bifacial Solar Cell, PC1D simulation

1. Introduction

Bifacial solar cell is a symmetric solar cell configuration in which sunlight is harnessed from both front and rear surfaces. Bifacial solar cells are attractive because they represent an elegant solution to enhanced output at lower material costs. There are several advantages of the bifacial solar cell configuration including lower temperature coefficient, capability to process thinner wafers, and ease of packaging both n and p type wafers in the same module. In some application environments, bifacial solar cell has an advantage since it works well in vertical configuration. This is, in contrast, with monofacial solar cells, which are often used at fixed angles. Therefore, bifacial solar cell can be implemented as structural component, i.e., fence or wall in building integrated photovoltaic systems. Similarly, bifacial solar cell panels can be mounted easily over carports, canopies, and other types of coverings.

The amount of power produced from the rear side of a bifacial solar cell is a function of the amount of sunlight incident on it. Thus, reflector or mirror should be appropriately placed on the backside of a bifacial solar module. The sunlight directed into the rear surface can potentially provide an additional light source to generate current almost identical to that of the front surface.

There are countless numbers of fabrication in bifacial solar cell. A few works has been reported modeling of bifacial solar cells using Matlab Simulink and PC1D. Mbodji *et al.* 2006 presented a theorical study of bifacial solar cell (n^+pp^+) under constant magnetic field and under constant illumination using Matlab Simulink. The effect of the magnetic field on both photocurrent and photovoltage has been described for each illumination mode.

Fateha *et al*., 2001 investigated a bifacial solar structure in order to achieve maximum output power. Their design featured a symmetrical structure consisting of two sub-cells on the front and rear surfaces using Matlab Simulink. They optimized the thickness of each sub-cell and varied back illumination ratios. They observed that the optimum thickness decreases with increase of rear surface illumination ratio based on the electrical mismatch between the two sub-cells.

Mihailetchi *et al.*, 2007 reported on n-type silicon solar cell with Al back junction using PC1D software. They focused on n^+np^+ configuration and varied the surface recombination velocity in order to enhance the front side performance. Higher efficiency, namely 17.5% was demonstrated after material optimization, higher wafer resistivity and increased lifetime. Using PC1D simulation software, You Lee 2004 observed that following boron diffusion, diffusion length was degraded. He was assumed that this was attributed to the impurities or contamination from the boron dopants diffused into the bulk of silicon material during high temperature thermal process.

In this study, a detailed description of bifacial solar cell based on PC1D simulations has been carried out. The structure of npp^+ was selected for all simulations. This choice was made due to the excellent results obtained from this structure. This structure is the simplest structure, most widely used method, is highly accurate and can be adapted for all types of solar cells. PC1D has been chosen as a simulation tool for this research regarding its user-friendly system. PC1D is the most common and perhaps simplest simulation software. The process

parameters can be adjusted by choosing the appropriate layers or contacts in the schematic diagram of the device. PC1D is usually used for solving the one-dimensional semiconductor equations based on Shockley–Read Hall recombination statistics (Shui-Yang *et al.* 2009). Based on these considerations, PC1D was chosen to describe bifacial solar cell in this study.

2. Simulation by PC1D

Computer-based simulations play a critical role in the design, development, and functionality of solar cells. Device modeling techniques substantially reduce the time and costs through optimization of process steps, choice of materials, and wafers. In this study, solar cell devices have been modeled using actual physical device configurations. This paper focuses on optimization of npp^+ configuration bifacial solar cells by employing PC1D simulations. Fig.1 schematically describes the bifacial solar cell configuration and identifies the process parameters impacting the performance of the device.

In accordance with Fig.1, critical process parameters investigated include emitter doping, bulk doping, minority carrier lifetime, wafer thickness, back surface doping, front and rear surface recombination and illumination from front and rear surfaces. These studies lead to a deeper understanding of the solar cell parameters impacting its performance. The optimized process parameters can then be the starting point in solar cell fabrication process.

Using PC1D software, a working model of the bifacial solar cell was developed in order to investigate the influence of process parameters identified above. Table 1 summarizes the process parameters in basic working model. The constant parameters in this simulation were base resistance, internal conductor and light intensity that were set at 0.0015 Ω, 0.3 S and 0.1 W/cm^2, respectively. The spectrum that used in this model was AM1.5 G. During the simulations, all the parameters were adopted as the default values except for the specific declared ones.

3. Results and Discussions

In this study detailed simulation studies of I-V characterization of bifacial solar cells have been carried out in order to get more insight into the factors determining the bifacial solar cell performance. The most critical part in this cell structure is the preparation and optimization of the emitter and back surface field (BSF) layer. In order to develop a deeper understanding of the physics of this device we carefully analyzed emitter, bulk and BSF layer and studied the variation of the cell parameters. The attention has been focused on the role of the minority carrier lifetime for the device performance.

3.1 Optimization of Emitter Doping Level

Diffusion to form p-n junction is perhaps the most critical step in solar cell fabrication. Based on experimental process parameters such as temperature, time, gas flow rate, configuration, doping level can vary over a wide range. Therefore, it is important to understand its influence on efficiency. For PC1D simulations, the emitter doping level was varied from 2.87E17 to 2.87E21 cm^{-3}; these values are well within experimentally observed values.The wafer p-type doping level has been kept constant at 1.513E16 cm^{-3} for all simulations. The performance variation as a function of emitter doping level have been shown in Fig.2.

From the figure, it can be seen the similar trends of the curve for open circuit voltage (V_{oc}), fill factor (FF) and efficiency. The curve are gradually increased from the emitter level of 2.87E17 to 2.87E20 cm^{-3} and decrease at the heavily doped emitter, namely 2.87E21 cm^{-3}. Meanwhile, the different has been seen in the current density (J_{sc}) curve. For a front side, the J_{sc} values are constant until the doping level of 2.87E20 cm^{-3}, then at highest emitter doping level, the J_{sc} are rapidly decrease. However, the J_{sc} values for backside are constant for all emitter doping level.

The highest efficiency is observed for the emitter doping of 2.87E20 cm^{-3}. The efficiency for the front side increases with the increasing emitter concentration. The front side efficiency values were 14.55 %, 15.44%, 16.22 %, and 16.37 % as the doping level increases from of 2.87E17 to 2.87E20 cm^{-3}. However, at the doping level of 2.87E21 cm^{-3}, the efficiency starts to decrease presumably due to recombination in the heavily-doped emitter layer. Similar trend is observed for the rear side. The emitter doping level strongly influences the V_{oc}, with relatively little impact on I_{sc}.

These performances can be explained by sheet resistance values. The sheet resistance of the emitter is an essential process control parameter. The relationship between sheet resistance and junction depth has been summarized in Table 2. For lightly doped emitters, large sheet resistances lead to high series resistance and poor fill factors. Additionally, the heavily doped emitter is considered as a dead layer with very high carrier recombination. The heavy diffusion limits the V_{oc} in solar cell performance (Cueves 2005). Therefore, cell efficiency is poor for both low and high emitter doping levels.

According to Markvart 2005, high doping narrows the bandgap. As doping level exceeds around 1E19 cm^{-3}, the effective bandgap of silicon is reduced. This results in an increase in intrinsic carrier concentration, n_i as well as the current density. Therefore, increasing doping to increase V_{oc} becomes counter-productive after a certain limit is reached. It is also important to note that, the representative values of emitter-saturation current density, J_{oe} for industrial n^+ region and p^+ diffusions are 8 x 10^{-13} Acm^{-2} and 5 x 10^{-13} Acm^{-2} respectively. The J_{oe} value from our simulations for an emitter concentration at 2.87E20 cm^{-3} and p-type wafer of 1.513E15 cm^{-3} are 3.47 x 10^{-13} Acm^{-2} and 5.627 x 10^{-14} Acm^{-2} respectively. These values are similar to the industrial standard. From the simulations, it is apparent that the sheet resistance value for the highest efficiency bifacial solar cell is 50 ohm/sq for the emitter concentration of 2.87E20 cm^{-3}. This value is in good agreement with high efficiency solar cells reported in journals (Markvart 2005).

3.2 Optimization of Bulk Doping Level

The Si wafer doping level also plays a critical role in cell performance. The wafer doping concentration influences the emitter and BSF doping level for junction formation. For simulations reported here, the emitter and BSF concentrations were kept constant at 2.87E20 cm^{-3} and 1E20 cm^{-3} respectively while the bulk doping level was varied from 1.513E15 to 1.513E20 cm^{-3}. Fig.3 plots the efficiency as a function bulk doping.

From Fig.3, it is observed that efficiency increases slowly to a maximum value at a concentration of 1.5E15 cm^{-3}, and then decreases rapidly at the bulk concentration of 1.51E18 cm^{-3} for the front side. For the rear surface, efficiency variation is relatively invariant up to bulk concentration of 1.51E16 cm^{-3} after which decreases rapidly; the highest efficiency is achieved at the bulk doping of 1.513E15 cm^{-3}. Higher doping concentrations lead to higher carrier recombination or reduced minority carrier lifetime. According to Goetzberger et al., 1998, for doping less than 10^{17} cm^{-3}, typical for most Si devices, radiative recombination plays virtually no role, and carrier lifetime is determined by the impurity level. While for a doping level greater than 10^{18} cm^{-3}, the Auger recombination become dominant. Since Auger process is assigned as lifetime, the relationship obtained empirically by Kendall (Goetzberger et al. 1998) is frequently used at the moment, accordingly, to which the lifetime in this range is calculated as;

$$\tau = \frac{\tau_o}{1 + \frac{N_D}{7E15}} \qquad \text{(Eq. 1)}$$

In this equation the carrier lifetime τ_o in pure, undoped silicon was assumed to be 400 µs. Therefore, it is clear that the higher the doping concentration, the recombination is more probable.

The bulk concentration significantly influences the emitter and BSF doping profiles. Table 3 summarizes the change in junction depth of emitter and BSF as a function of bulk doping level. The highest junction depth for emitter and BSF is observed at the lowest doping level of Si wafer. Cueves 2005 proposed that the resistivity and subsequently bulk doping concentration is a critical factor in the optimization of the fabrication process as well as the interpretation of solar cell performance, since both the V_{oc} and the I_{sc} exhibit strong dependence on it. The lifetime and the diffusion length are also correlated to the resistivity of the substrate, with lower bulk resistivity wafers usually characterized with lower lifetime. Therefore, performance loss at higher bulk concentrations is largely due to significant reduction in minority carrier lifetime.

Typical value of resistivity for p-type Si wafer used in industrial manufacturing is 0.5-3 ohm-cm. From the simulated value of resistivity, it can be determined that for the bulk Si with a doping level of 1.513E15 and 1.513E16 cm^{-3}, resistivity falls in this range. The good resistivity value for a Si wafer with a doping level of 1.513E15 and 1.513E16 cm^{-3} varies from 0.1 ohm-cm and 1.0 ohm-cm, respectively.

Therefore, in accordance with simulations described above, it can be argued that the Si wafer with a doping concentration of 10^{15} to 10^{16} cm^{-3} should be used in the fabrication of bifacial solar cell.

3.3 Optimization of Back Surface Field (BSF) Doping Level

BSF is one of the most important regions in a bifacial solar cell. The BSF doping level was varied from 10^{16} to 10^{20} cm^{-3} while keeping the emitter doping level at 2.87E20 cm^{-3} and bulk concentration at 1.513E15 cm^{-3}. Fig.4 plots J_{sc}, V_{oc} and efficiency as a function of BSF doping level for front and back surface. It is observed that key solar cell parameters increase rapidly as doping level is increased to 1.5E20 cm^{-3}; at higher doping concentrations, performance decreases rapidly.

From Fig. 4, it is observed that J_{sc} and efficiency show the similar response for the rear surface of bifacial solar cell. Both J_{sc} and efficiency increase until the doping level of 10^{19} cm^{-3} is reached, and then rapidly decrease at the doping levels of 10^{20} and 10^{21} cm^{-3}. The highest V_{oc} is observed at the BSF doping level of 10^{19} cm^{-3} and exhibits only a slight decrease at the doping level of 10^{20} cm^{-3}. It is interesting to see that the V_{oc} value for front

and rear surface of bifacial solar cell is almost identical at 0.6296 and 0.6284 V respectively at doping level of 10^{19} cm^{-3}.

Table 4 summarizes the junction depth and sheet resistance as a function of BSF doping. BSF with a doping of 10^{19} and 10^{20} cm^{-3} exhibits a practical value of sheet resistances of 107.8 ohm/sq and 19.96 ohm/sq respectively. Higher sheet resistance leads to larger contact resistance which will reduce cell V_{oc}. High resistivity makes the solar cell more independent of the quality of the surfaces (Cueves 2005). The thickness of the BSF or p^+ layer is an essential parameter to achieve an optimized pp^+ interface with low surface recombination velocity (Szlufcik et al. 2005). The difference in thickness between a shallow and highly doped BSF is approximately 2 μm.

Variation of bifacial solar cell efficiency as a function of Si wafer thickness and minority carrier lifetime at shallow (10^{16} cm^{-3}) and heavily-doped (10^{20} cm^{-3}) BSF layer has been carried out in order to determine lower and upper performance limits. Fig. 5 and 6 summarize key solar cell parameters at low (10 μs) and high (1000 μs) lifetime for shallow and highly doped BSF.

From Fig. 5, it is observed that front side efficiency increased while backside efficiency decreases with increasing thickness. High lifetime wafers exhibit superior performance than low lifetime. For thin wafers, the performance of low lifetime and high lifetime solar cell is comparable. As the thickness increases, the efficiency gap between high and low lifetimes becomes significant. From these simulations, it can be argued that, for a shallow-doped BSF, thinner wafer is required in order to achieve comparable performance from front and rear surfaces of the bifacial solar cell independent of its lifetime value.

Fig.6 plots efficiency of low and high lifetime wafers as a function of thickness for heavily-doped BSF for (a) front and (b) back surface. From the plotted results, it is noted that for a low lifetime Si wafer, the performance of the rear surface is poor. This is in contrast with the high lifetime wafer, where the rear surface performance is comparable to a low lifetime wafer for a front side at the thickness of 100 μm and 150 μm.

For both shallow and heavily doped BSF, it is noted that the heavily doped BSF exhibits superior performance in comparison with shallow-doped BSF for both low and high lifetime Si wafers. It can be summarized that either heavy or shallow doped BSF, comparable performance can be achieved for thin and high lifetime Si wafers.

3.4 Influence of Surface Recombination Velocity

Recombination of electrons and holes also occurs at the solar cell surfaces. The speed at which electron-hole pairs recombine at the surface is called the surface recombination velocity, S. Firstly, the performance variation with respect to front surface recombination velocity, S_f is carried out. The back surface recombination velocity, S_b is kept constant at 10^4, while S_f is varied at 10^2 to 10^6 cm/s. For convenience, this variation is carried out at a high minority carrier lifetime Si wafer, namely 1000 μs.

Fig.7 plots the simulated efficiency versus S_f for four thicknesses of the bifacial solar cell. Since the performance of 10^2 and 10^3 cm/s of S_f was observed to be identical, the plotted data only exhibits the performance from S_f at 10^3 to 10^6 cm/s. As expected, efficiency is reduced as S_f is increases. Both front and rear surfaces exhibit similar response. The highest efficiency achieved by front and back surfaces of bifacial solar cell are 16.84% and 14.32% respectively. From the simulated response in Fig.7, can be argued that, at the high minority carrier lifetime, the S_f must be in a range of 10^3 and 10^4 cm/s. Highest value of S_f make the recombination faster, therefore the high S_f shows the lower efficiency. In comparison, the performance as a function of S_b is different. Back surface recombination velocity is varied from 10^2 to 10^6 cm/s while S_f is constant at 10^5. Fig.8 plots the calculated efficiency versus S_b for four thicknesses of the bifacial solar cell. It is clearly observed that the rear surface contact is significantly impacted with the change in S_b, while the front surface efficiency exhibits little efficiency of 15.5 % to 16.45 %. The thinner the solar cell, the stronger is this effect.

This simulation indicates that in order to achieve high efficiency bifacial solar cell, the S_b should be in 10^2 to 10^3 cm/s range. These results also suggest that superior surface passivation layers should be deposited to improve the performance from the rear surface. This is by virtue of reduction in the recombination of electron and holes at the surface.

4. Conclusion

All the process parameters that potentially influence the bifacial solar cell performance have been investigated, It was observed that the best doping for emitter, bulk and BSF were 2.87E20 cm^{-3}, 1.513E15 cm^{-3} and 1E20 cm^{-3}respectively. For the minority carrier lifetime, even though the 10,000 μs exhibits the highest performance, for most of the studies for this parameter, focus was on 10-1000 μs, which were closer to the practical values. The optimum wafer thickness for high efficiency bifacial solar cells was determined to be in ~ 150-200 μm

thickness range. The best combinations of front and rear surface recombination velocity were 10^5 and 10^4 cm/s, respectively.

From these simulation results, the assumptions on what type of Si wafer to be used, the best concentration for each layer, and the choice of materials to be used were determined. In a fabrication process, for the case of emitter concentration, BSF doping level, reflectivity, temperature and wafer thickness, these parameters can be adjusted in accordance with modeled values. In a real case, the thinning process can be done to thin down the thick Si wafer. In order to adjust process parameters relating to concentration, layer thickness, sheet resistance value, resistivity and junction depth; experimental conditions including furnace temperature, gas flow rate, gas ratios, and combination of chemical and deposition times are optimized. However, it is critically important to note that the minority carrier lifetime cannot be controlled since it depends on the wafer used for fabrication. Therefore, further research on fabrication of bifacial solar cell and comparison of experimental and simulation results will be carried out in the future.

References

Cueves, A. (2005). Characterisation and Diagnosis of Silicon Wafers and Devices, in : Tom Markvart, Solar Cells: Materials, Manufacture and Operation, Elsevier Ltd., UK, pp. 164 – 214.

Fateha, M.Y., Eldalal, G.M., & Soliman, M.M. (2001). Optimum design for bifacial silicon solar cells. Renewable Energy. 22, 269-274.

Goetzberger, A., Knobloch, J., & Voss, B. (1998). Crytalline Silicon Solar cell, Wiley, Germany.

Markvart, T. 2005. Solar Cells: Materials, Manufacture and Operation, First edition, Elsevier Ltd., UK.

Mbodji, S., Ly Diallo, A., Ly, I., Barro, F.I, Zougmore, F., & Sissako, G. (2006). Equivalent electric circuit MATLAB Simulink of a Bifacial Solar Cell in Transient State. Applied Magnetic Field Effect. J.Sci., 6, 99-104.

Mihailetchi, V.D., Geerligs, L.J., Komatsu, Buck, T., Rover, I., Wambach, K., Knopf, C., Kopecek, & R. (2007). High efficiency industrial screen printed n-type mc-Si solar cells with front boron emitter. 22nd European Photovoltaic Solar Energy Conference, 1581–1584.

Shui-Yang Lien & Dong-Sing Wuu. (2009). Simulation and Fabrication of Heterojunction Silicon Solar Cells from Numerical Computer and Hot-Wire CVD. Prog. Photovolt: Res. Appl. DOI: 10.1002/pip.

Szlufcik, J., Agostinelli, G., Duerinckx, F., Kerschaver, E.V, & Beaucarne, G. (2005). Low Cost Industrial Technologies of Crystalline Silicon Solar Cells, in : Tom Markvart, Solar Cells: Materials, Manufacture and Operation, Elsevier Ltd., UK, pp. 89-120.

You Lee, J. (2004). Boron Back Surface Field Using spin on dopants by rapid thermal processing. Journal of Korean Physical Society, 44(6), 1581-1586.

Suhaila Sepeai is a Research Fellow at Solar Energy Research Institute (SERI), Universiti Kebangsaan Malaysia since 2008. She obtained her Bachelor Science in Physics (2005) and MSc. in Microelectronics Engineering from Universiti Kebangsaan Malaysia (2008). Currently, she is in final year of PhD study in Universiti Kebangsaan Malaysia. Her PhD researches on the fabrication of nano-textured and thin silicon bifacial solar cells. Her research interests include fabrication of photonic device, device simulation and thin film technology. She is a member of Malaysian Solid State Science and Technology Society (MASS).

Saleem H.Zaidi is a Principal Research Fellow at Solar Energy Research Institute (SERI), Universiti Kebangsaan Malaysia since 2010. He obtained his PhD in Physics from University of New Mexico in 1989. He obtained his MSc. in Physics from Michigan State University in 1984, and BSc. in Physics from Quaid-i-Azam University, Pakistan in 1982. He also the founder, CEO and Chief Scientist of Gratings Inc., USA from 200-2010. He is a co-author of 17 US-patents. His main contributions are in Advanced Silicon Solar Cell and Advanced Thin Film Solar Cell.

M.K.M.Desa is a Lecturer at the School of Electrical and Electronic Engineering, Universiti Sains Malaysia (USM), Nibong Tebal, Pulau Pinang. He obtained his MEng. and BSc. in Electrical Electronic Engineering from Loughborough University, UK in 2008 and 2007 respectively. Currently, he is pursuing PhD research in Back Contact Silicon Solar Cell at Solar Energy Research Institute (SERI) UKM.

M.Y.Sulaiman is a Principal Research Fellow at Solar Energy Research Institute (SERI), Universiti Kebangsaan Malaysia. He obtained his PhD in Radiation Physics from University of London in 1977. He received his BSc. in Applied Physics and Physics from University of Malaya in 1973 and 1972 respectively. His research interests includes third generation solar cells; preparation using hydrothermal, electro-deposition and chemical bath

deposition, Fabrication and characterization of monosilicon solar cell, installationofsolarsystem, solar cooler, Quantum information, embedded system, switched reluctance motor design, design and development of alkali metal to thermal energy converter, solar powered refrigerator using stirling cooler.

K. Sopian is the Director of the Solar Energy Research Institute (SERI), a centre of excellence for the research and development in solar energy technology in UKM. He obtained his BSc. in Mechanical Engineering from the University of Wisconsin-Madison in 1985, MSc. in Energy Resources from the University of Pittsburgh in 1989 and PhD in Mechanical Engineering from the Dorgan Solar Laboratory, University of Miami in 1997. He is presently the Professor in Renewable Energy at the Department of Mechanical and Material Engineering, UKM. His main contributions are in solar radiation modelling, alternative material for solar absorber, solar water heating system with integrated storage system, solar desalination, solar cooling, day lighting using solar light pipes, solar assisted drying systems, grid-connected photovoltaic system, combined photovoltaic thermal or hybrid collector and solar hydrogen production system.

N. A.Ludin obtained PhD in Chemistry from University of Wales, Bangor, UK. Currently, she is a Senior Research Fellow at the Solar Energy Research Institute, UKM. She engages in research in education in solar photovoltaic technology, advanced materials for solar cells and renewable energy policy. Her postgraduate supervision and research currently focuses on green technology of solar photovoltaic, especially related to thin film and dye-sensitized solar cells, materials study for solar cells and solar cells modelling and simulation. She also involved in developing and implementing the BioGen UNDP project (2000-2007) for promoting the RE resources and technologies and formulating RE policy, tariff and financing in Malaysia.

M.Adib Ibrahim is a Research Fellow at the Solar Energy Research Institute (SERI), Universiti Kebangsaan Malaysia since 2006. He received his Bachelor Science in Chemical Engineering from the Universiti Teknologi Malaysia. He holds Master in Business Administration and MSc. in Chemical and Process Engineering from Universiti Kebangsaan Malaysia (UKM). Currently, he is waiting for PhD thesis defence in University of Southampton, UK. His PhD researches on development of light harvesting materials on the silicon for solar photovoltaic application. He also develops theoretical study on the energy conversion of photosynthesis which has similarities of energy transfer in photovoltaic system.

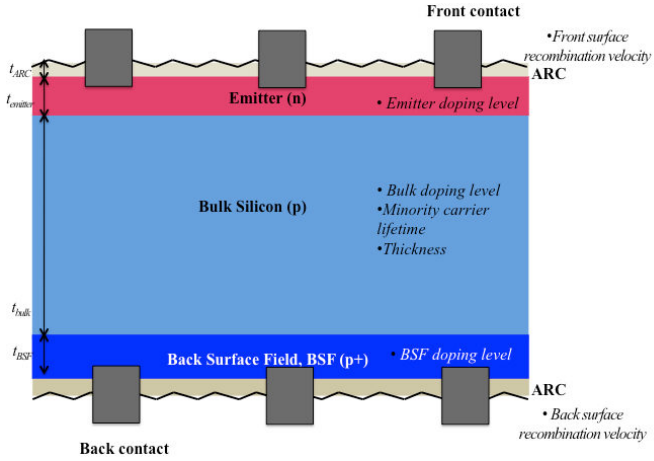

Figure 1. Bifacial Solar Cell Configuration and Relevant Process Parameters at Respective Interfaces

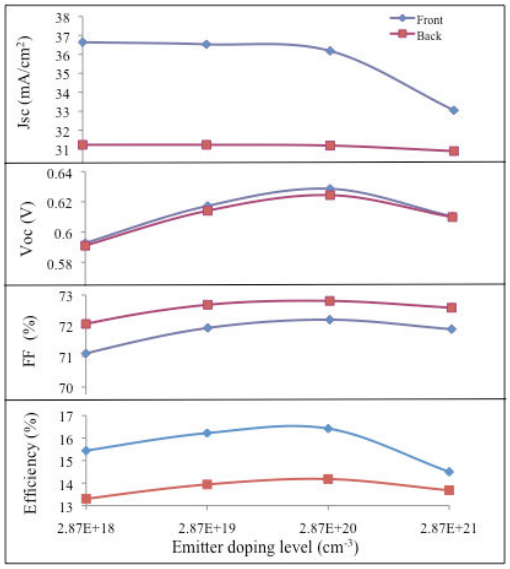

Figure 2. The J_{sc}, V_{oc}, FF and Efficiency as Functions of Emitter Doping Level

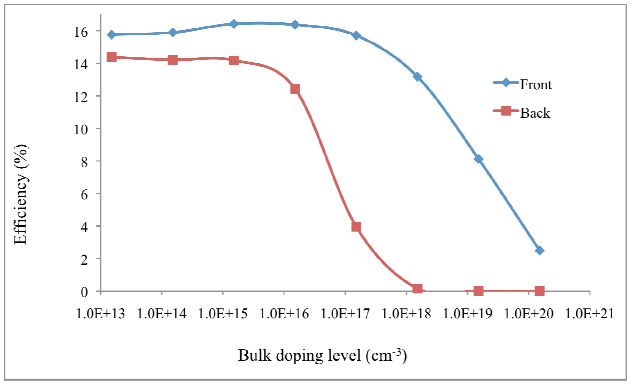

Figure 3. Efficiency Variation as a Function of Wafer Doping Level

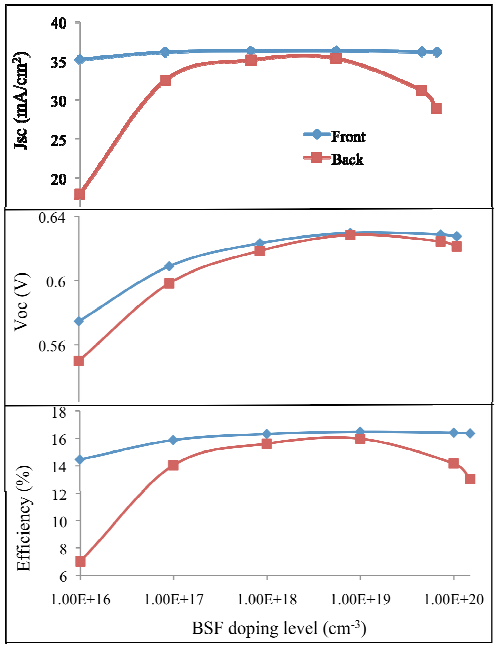

Figure 4.The J_{sc}, V_{oc} and Efficiency as Functions of BSF Doping Level

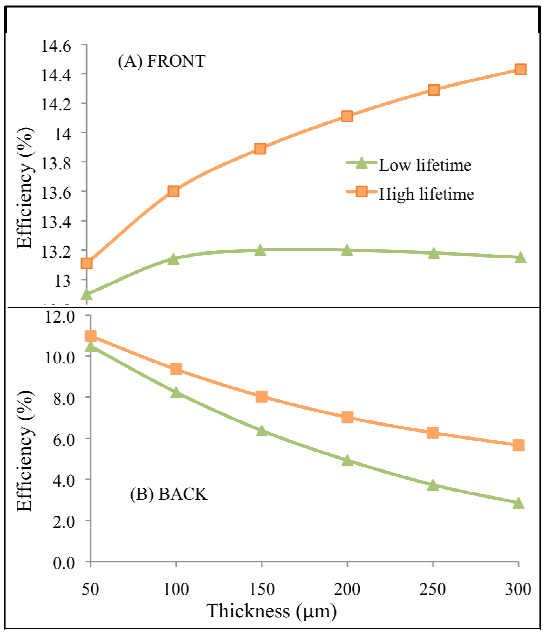

Figure 5. Bifacial Solar Cell Efficiency as a Function of Thickness for Low (10 μs) and High Lifetime (1000 μs) Wafers with Lightly Doped (10^{16} cm^{-3}) BSF

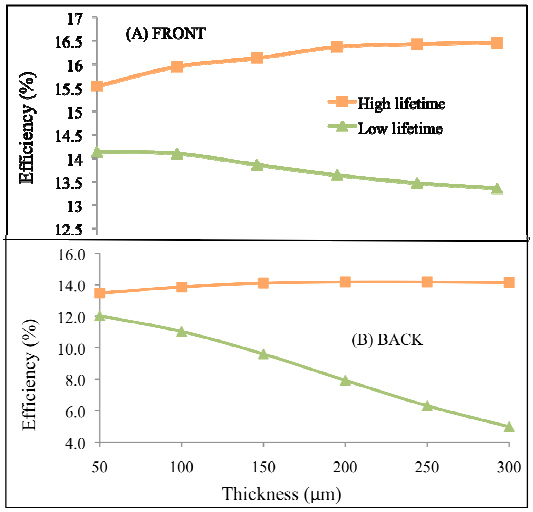

Figure 6. Bifacial Solar Cell Efficiency as a Function of Thickness for Low (10 μs) and High (1000 μs) Lifetime Wafers with Heavily-Doped (10^{20} cm^{-3}) BSF for (a) Front and (b) Back Surface

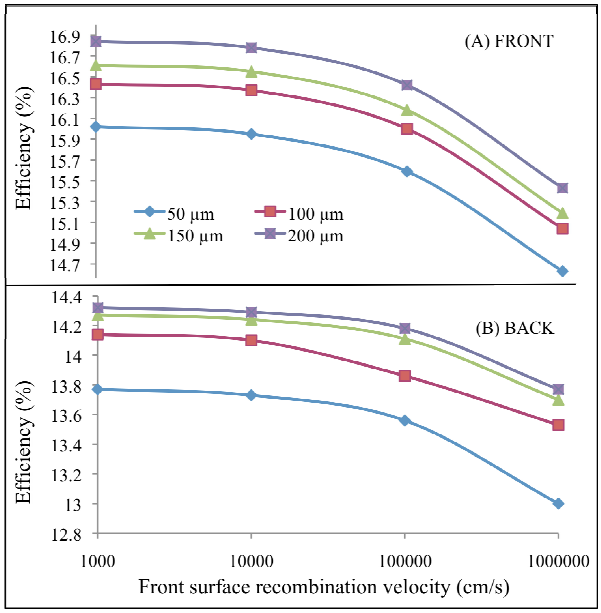

Figure 7. Bifacial Solar Cell Efficiency Variation as a Function of S_f for Increasing Wafer Thicknesses for (a) Front and (b) Back Side

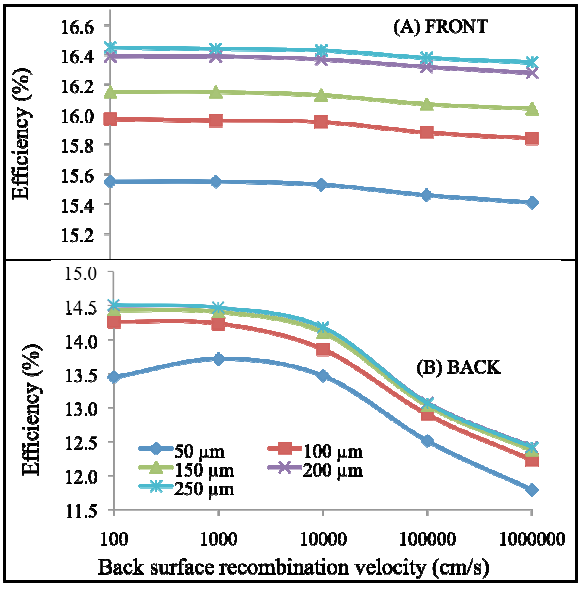

Figure 8. Bifacial Solar Cell Efficiency Variation as a Function of Back Surface Recombination Velocity for Increasing Wafer Thicknesses for (a) Front and (b) Back Surface

Table 1. Process parameter for the bifacial solar cell model

Process Parameter	Value and unit
Device area	100 cm^2
Front surface texture depth	3 μm/ 54.74°
Rear surface texture depth	3 μm/ 54.74°
Front / Rear surface coating	SiN - 70 nm
Internal / external optical reflectance	10%
Base contact	0.015 Ω
Internal conductor	0.3 S
Thickness	200 μm
Material	Silicon (Si)
Carrier mobilities for electron and holes (μ_e / μ_h)	1450 cm^2/Vs 413 cm^2/Vs
Dielectric constant	11.9
Band gap	1.124 eV
Intrinsic conc. At 300K	1E10 cm^{-3}
Absorption coefficient	Silicon
Free carrier absorption enabled	Yes
P-type background doping	1.513E15 cm^{-3}
1st front diffusion: n type	2.87E20 cm^{-3}
2nd front diffusion	-
1st rear diffusion: p type	1E20 cm^{-3}
Bulk recombination	1000 μs
Front surface recombination	1E5 cm/s
Rear surface recombination	1E4 cm/s
Temperature	25°C
Base circuit	-0.8 to 0.8 V
Collector circuit	Zero
Light source	Front/Rear
Constant intensity	0.1 W/cm^2
Spectrum	AM 1.5G

Table 2. Junction depth and sheet resistance variation with emitter doping

Emitter doping (cm^{-3})	Junction depth (μm)	Sheet resistance (ohm /sq)
2.87E+17	0.2069	5611
2.87E+18	0.2571	1340
2.87E+19	0.2999	313
2.87E+20	0.3378	50
2.87E+21	0.3721	5.83

Table 3. Junction depth and resistivity variation with bulk doping

Bulk doping (cm^{-3})	Junction depth (μm)		ρ (ohm-cm)
	Emitter	BSF	
1.51E+13	0.4037	3.71	879.2
1.51E+14	0.3721	3.401	88.41
1.51E+15	0.3378	3.06	9.058
1.51E+16	0.2999	2.679	0.9997
1.51E+17	0.2571	2.243	0.1392
1.51E+18	0.2069	1.718	0.02803
1.51E+19	0.1437	1.015	0.006019
1.51E+20	0.0469	-	0.0009184

Table 4. Junction depth and sheet resistance variation with BSF doping

BSF doping (cm^{-3})	Junction depth (μm)	Sheet resistance (ohm/sq)
1E16	1.015	27730
1E17	1.718	3096
1E18	2.243	509.1
1E19	2.679	107.8
1E20	3.06	19.96
1.5E20	3.122	14.31